Generation of ultrashort pulses by four wave mixing in a gas-filled hollow core fiber

OPEN ACCESS

Made open access 18 February 2019

IOP Publishing

Journal of Optics

J. Opt. **20** (2018) 125503 (9pp)

https://doi.org/10.1088/2040-8986/aaec41

Generation of ultrashort pulses by four wave mixing in a gas-filled hollow core fiber

Anna G Ciriolo, Aditya Pusala, Matteo Negro, Michele Devetta, Davide Faccialà, Giacomo Mariani, Caterina Vozzi and Salvatore Stagira

Instituto di Fotonica e Nanotecnologie IFN-CNR & Dipartimento di Fisica, Politecnico di Milano, Piazza Leonardo da Vinci 32, I-20133 Milano, di Fotonica e Nanotecnologie IFN-CNR & Dipartimento di Fisica, Politecnico di Milano, Italy

E-mail: annagabriella.ciriolo@polimi.it

Received 11 July 2018, revised 14 September 2018
Accepted for publication 3 October 2018
Published 14 November 2018

Abstract

The four wave mixing (FWM) process is widely exploited for the generation of tunable ultrashort light pulses. Usually this process is driven in bulk materials, which are however prone to optical damage at high pump laser intensities. A tunable source of ultrashort 10 μJ level pulses in the visible spectral region is described here. In particular, we report on the implementation of FWM driven by a two-color ultrafast laser pulse inside a gas-filled hollow core fiber (HCF). Due to the high-damage threshold and the long interaction distance, the HCF-based FWM configuration proves to be suitable for high-energy applications. Moreover, this technique can be potentially used for ultrashort pulses generation within a wide range of spectral regions; a discussion on the possibility to extend our scheme to the generation of few-cycle mid-IR pulse is provided.

Keywords: nonlinear wave mixing, nonlinear optics, parametric processes, ultrafast nonlinear optics

(Some figures may appear in colour only in the online journal)

1. Introduction

Over the last few decades, the development of ultrafast laser sources led to remarkable advances in the field of spectroscopy, providing a powerful technology for studying atomic, molecular and solid state dynamics on an ultrashort time scale [1]. Currently, the increasing interest in strong field physics and the great attention on the wavelength-scaling law underlying matter response under a strong-field excitation are driving laser technology towards novel frequency regimes. The leading approach for high-energy wavelength-tunable ultra-broadband pulse generation is provided by optical parametric amplification (OPA). Unlike stimulated emission in active media, parametric amplification is a non-resonant process that involves energy transfer from a high-energy high-frequency pump to low-energy low-frequency beams, the signal and the newly generated idler. By overcoming the restrictions due to the linewidth of electronic or vibrational lasing transitions, OPA allows for broadband amplification in a wide range of spectral regions provided that proper phase-matching occurs between the spectral components of the pump and signal/idler fields. The pump-to-signal conversion efficiency of the parametric sources is commonly between 10% and 30%, and to achieve high output energies, extremely intense sources, up to the multi-terawatt scale, must be used as pump. Moreover, the OPA scheme provides both energy and bandwidth scalability. Nowadays, tunable few-cycle pulses with an energy above the μJ-level can be generated in the visible and in the infrared (IR) by means of this technique [2, 3]. A mJ-level BBO-based parametric amplifier at 1.5 μm was demonstrated in 2007 by Vozzi *et al*, providing 10 Hz 1.2 mJ, 17 fs CEP-stable pulses at 1.5 μm [4]. Even shorter durations were achieved by spectral broadening of the OPA output pulses. Sub-two-cycle hundreds-of-μJ 1 kHz OPA pulses at 2 μm were generated by Hauri *et al* in 2007 [5] through self-phase modulation (SPM) in a plasma filament. By a gas-filled HCF as an alternative to plasma, a 1.6-optical cycle duration was achived by Schmidt *et al* in 2011 [6].

A promising route towards the development of parametric system on a multi-mJ scale is represented by optical parametric chirped pulse amplification (OPCPA). OPCPA provides the possibility to attain amplification up to energy levels that are inaccessible by standard OPA systems because of the limitations imposed by optical damage. A main drawback of the OPCPA system is the considerable complexity of the experimental setup. In this framework, it is worth mentioning several outstanding results related to OPCPA systems operating in the mid-IR. In 2011, Andriukaitis *et al* achieved a mid-IR OPCPA system at a central wavelength of 3.9 μm that delivers few-optical-cycle 8 mJ pulses [7]. Mayer *et al* reported on the generation of sub-four-cycle 12 μJ pulses centered at 3.4 μm from an OPCPA working at 50 kHz [8]. Shamir *et al* implemented an OPCPA source that delivers of 2 μm pulses with an energy of 60 μJ and a repetition rate of 100 kHz [9]. In 2016, Sanchez *et al* reported a sub-eight-optical-cycle OPCPA system at 7 μm approaching mJ-level pulse energy at 100 Hz repetition rate [10]. More recently, Elu *et al* demonstrated the generation of 100 μJ 3 μm pulses at 160 kHz with a duration down to the single-cycle regime by OPCPA followed by soliton self compression inside a gas-filled photonic crystal fiber [11].

In this work, we explore a different approach to wavelength-tunable ultrashort pulses generation in the visible spectral region based on four wave mixing (FWM) inside a gas-filled hollow core fiber. FWM has attracted attention as a promising method for ultrashort pulse generation, providing the possibility for frequency-conversion in different portions of the spectrum. Wavelength-tunable ultrashort pulse generation has been achieved by means of FWM in bulk media, including CaF_2 and BaF_2 for wavelength conversion into the mid-IR [12], while BK7 glass, fused silica, and sapphire plates for wavelength conversion into the visible [13–15], and BBO for conversion into the UV [16]. FWM in single mode optical fibers has also been demonstrated [17]. In the case of optical fibers, nonlinear processes are strongly affected by chromatic dispersion. As a consequence, an efficient FWM has been obtained within the zero-dispersion wavelength region [18, 19]. Concerning ultrashort pulse generation, FWM has been demonstrated in microstructuted fibers [20], enabling the generation of an almost octave-spanning spectrum by cascaded FWM in the anomalous dispersion region [21].

In the case of bulk media, the possibility to extend both the OPA and the FWM schemes to several regions of the spectrum is limited by the availability of nonlinear crystals and glasses with a suitable optical transparency in the spectral window of interest. Moreover, the energy of the incoming laser pulses can be pushed up to the limit imposed by optical damage, thus strongly compromising the energy scalability.

With respect to bulk media, gas media exhibit a higher damage threshold upon optical excitation, making them a suitable target for frequency conversion processes driven by intense laser fields. On the other hand, the nonlinear optical response is commonly weaker in gas media than in bulk media. Moreover, since an unperturbed gas medium exhibits an isotropic response and its optical properties cannot be permanently engineered, as in the case of nonlinear crystals, birefringence or periodically poled arrangements cannot be used to optimize the phase matching. In addition, due to the low density, long interaction lengths are required in order to achieve high conversion efficiency. The implementation of a FWM experiment in gas media actually relies on the use of methods for confining the radiation on a distance longer than the confocal parameter of the laser beam. In this sense, plasma-sustained filamentation has been successfully exploited. Specifically, tunable few-cycle pulses in a number of spectral windows have been generated in a gas cell by means of FWM under a filamentation regime, including in the UV [22–25], the visible [26], the mid-IR [27–29] and also in the THz [30, 31]. The typical energy attained being on a sub-10 μJ scale. In order to increase the FWM signal energy, it is necessary to use a higher driving pulse energy. However, because of saturation effects in the intensity dependence [32], the filamentation method poses strong limitations towards energy scaling.

As an alternative to filamentation, a gas-filled capillary can be used for achieving the confinement. Indeed, UV pulses with temporal duration in the sub-10 fs scale were generated by means of cascaded FWM in a HCF filled with noble gases [22, 23]. The HCF-based approach offers several advantages with respect to filamentation. In particular, the interaction length corresponds to the waveguide length. The beam propagation is determined by the fiber modes such that the intensity and focusing geometry are not coupled as in filamentation. Moreover, the intensity may be increased up to the fiber damage limits. Additionally, the beam coming out from the guiding structure is endowed with a high spatial quality.

Here, we describe FWM performed inside a gas-filled HCF as driven by a two-color laser field composed of 800 nm pulses (ω_1) co-propagating with near-IR pulses (ω_2). Phase-matching is achieved for a three-photon combination sequence which leads to the generation of new components (ω_3) in the visible spectrum ($2\omega_1 - \omega_2 = \omega_3$). The broadband spectrum of the driving pulses allows the generation of a broadband visible spectrum associated to optical pulses with a duration of a few-tens of femtosecond and an energy above the μJ-level. In addition, numerical simulations under the same experimental conditions show a good agreement with the experimental measurements. By properly selecting the experimental parameters, ultra-broadband FWM generation in the mid-IR is also numerically predicted (the corresponding photons combination rule is $2\omega_2 - \omega_1 = \omega_3$ in this case), thus supporting the possibility to extend our scheme to long-wavelength pulse generation in the few-cycle regime.

2. Experimental methods and results

In our experiment, 60 fs 200 μJ 800 nm pulses provided by a 10 Hz Ti:sapphire (Ti:Sa) laser source were used in combination with 25 fs 300 μJ pulses delivered by an OPA system tunable from 1.3 to 1.9 μm [4]. The OPA is pumped by a 10 mJ portion of Ti:Sa laser output and it operates at the same repetition rate. The temporal and spectral properties of the

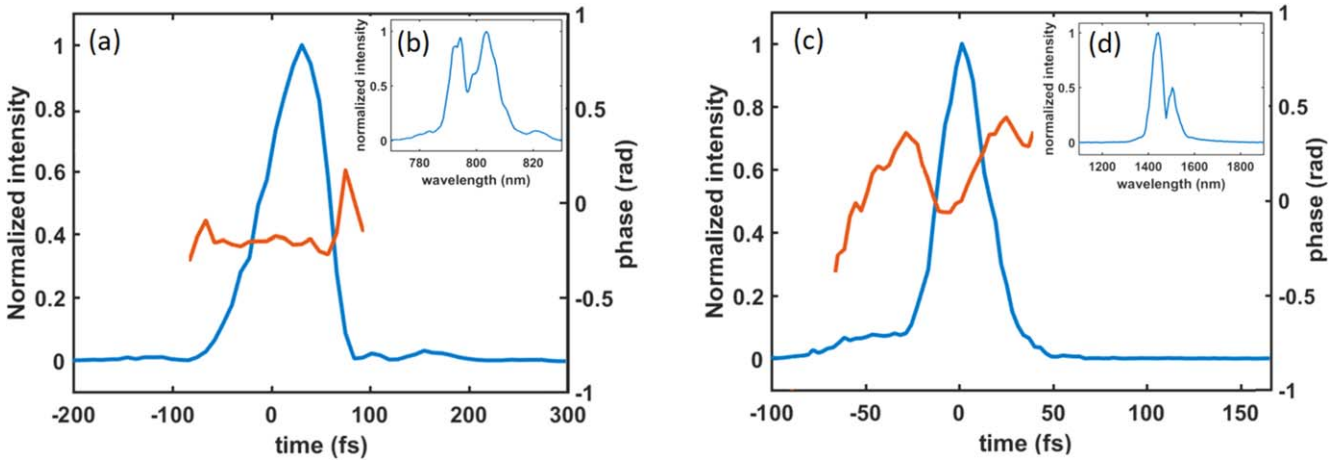

Figure 1. Temporal and spectral characterization of the input fields obtained by FROG measurements. (a) Temporal profile and phase of the 800 nm pulse. In the insert (b), the spectrum of the 800 nm field is shown. (c) Temporal profile and phase of the OPA pulse tuned at 1.45 μm. In the insert (d), the corresponding spectrum is reported.

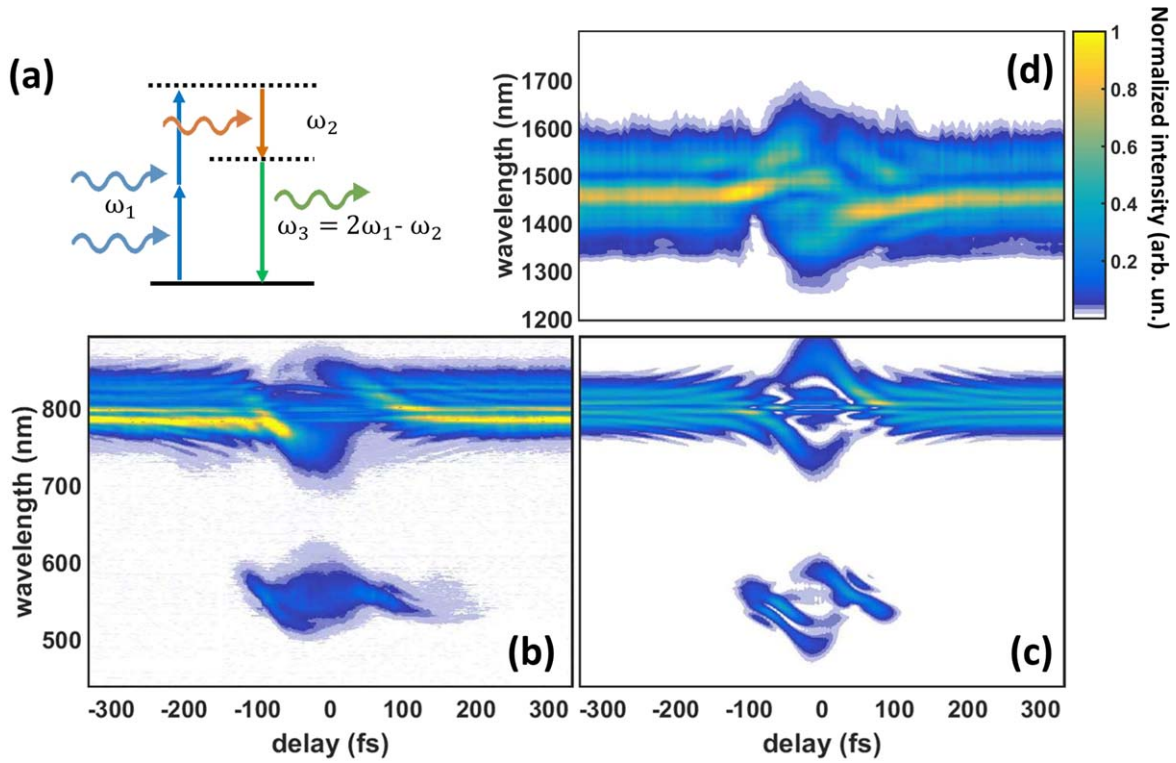

Figure 2. FWM generation in 400 mbra of Kr. (a) In the insert, the four-photon mixing sequence is reported. (b) Experimental measurement showing the 800 nm pulse spectra and FWM spectra as a function of the delay between the 800 nm and the 1.45 μm pulses. According to the convention used, the delay is negative (positive) when the 1.45 μm pulse arrives before (after) the 800 nm pulse. (c) FWM generation as predicted by numerical simulations performed in the same conditions as in the experiment. (d) Experimental measurement showing the 1.45 μm pulses spectra as a function of the delay of the 800 nm.

800 nm and of the OPA input fields are reported in figure 1. A detailed description of the sources is provided by Vozzi *et al* in [33].

The two beams with parallel polarization were collinearly combined by means of a dichroic mirror and were focused by means of a 60 cm focusing mirror inside a gas-filled 1 m long HCF with a inner diameter of 330 μm. The temporal delay between the 800 nm and the OPA pulses was controlled by means of a folded optical delay line with a motorized translation stage located on the 800 nm path. Several gases have been explored, including kripton (Kr), nitrogen (N_2) and carbon dioxide (CO_2). These media exhibit a high ionization threshold (above 10^{14} W cm^{-2} [34]) and a large third-order hyperpolarizability (on the order of 15×10^{-62} C^4 m^4 J^{-3} [35]), thus resulting ideal candidates for FWM by an intense driving radiation. A pressure regime lower than 1 bar was chosen, which ensures proper phase-matching conditions for the $\omega_3 = 2\omega_1 - \omega_2$ photon mixing combination. Indeed,

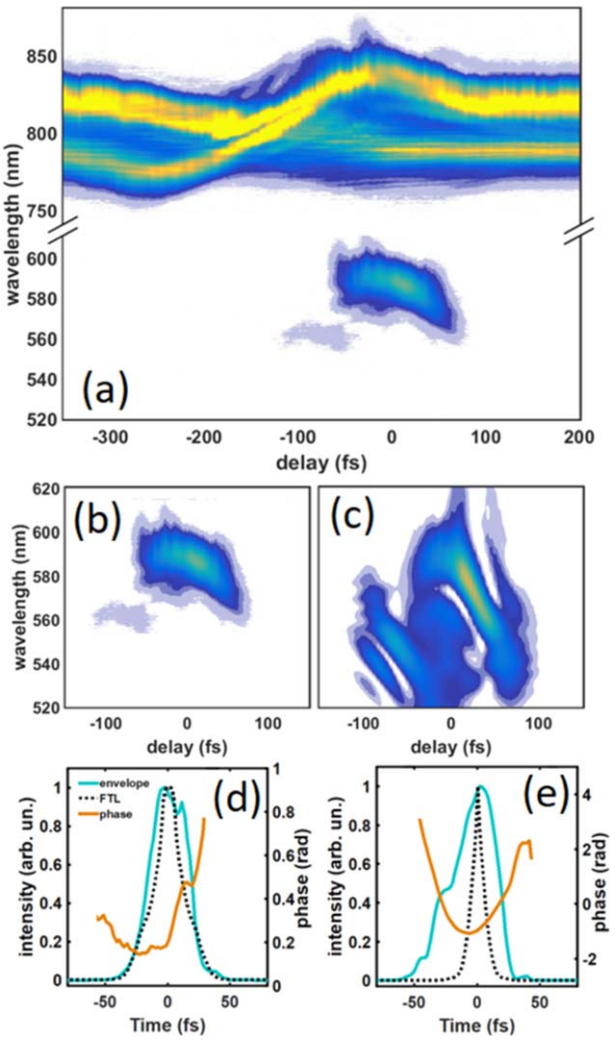

Figure 3. (a) Evolution of the 800 nm spectrum and of the FWM spectrum as a function of the delay between the two input fields. The OPA was tuned at 1.45 μm. The measurements were acquired at a CO_2 pressure of 400 mbar. FWM generation in CO_2: (b) as experimentally measured and (c) as theoretically predicted. FWM pulse temporal characterization: (d) resulting from SH FROG measurement and (e) resulting from simulations.

according to our calculations, at those pressures the phase-mismatch vector ($\Delta\mathbf{k} = \mathbf{k}_2 + \mathbf{k}_3 - 2\mathbf{k}_1$, with $\mathbf{k}$ wavevector) was assessed to be smaller than 3 m^{-1} over the whole range of tunability of the OPA system. Moreover, the velocity-mismatch among the pulses (estimated upon a multi-cycle pulse regime as $\delta_{13} = 1/v_1 - 1/v_3$ and $\delta_{23} = 1/v_2 - 1/v_3$, with v group velocity) turns out to be below 10 fs m^{-1}, meaning that a pulse walk-off less than 10 fs occurs during the propagation within the fiber.

In the above mentioned experimental conditions, FWM generation was achieved associated to the generation of new components in the visible spectral region. In figure 2, we report an experimental measurement obtained in Kr by tuning the OPA at 1450 nm. Figure 2(a) shows a sketch of the four photon interaction. A sequence of spectra detected at the HCF output as a function of the delay between the two driving pulses is shown in figure 2(b). According to our convention, the delay is negative (positive) when the OPA pulses come before (after) the 800 nm pulses. Two spectral contributions can be clearly identified. The contribution around 800 nm corresponds to that portion of the residual driving laser beam that exits from the HCF. The spectrum extends from 750 nm up to 850 nm because of SPM. Moreover, a strong perturbation in the shape of the 800 nm spectrum can be observed at around zero-delay when the temporal overlap is achieved between the 800 nm and the OPA pulses; this spectral perturbation is due the cross-phase modulation (XPM) [36, 37]. SPM and XPM correspondingly affect the OPA pulse spectrum as shown in figure 2(d). In the same delay window, a second contribution centered at 550 nm arises, which corresponds to the newly generated FWM signal. The FWM spectrum shows an evolution as a function of the delay that correlates to the perturbation of the driving fields spectra produced by the XPM. This effect cannot be avoided in a nonlinear regime and the FWM spectrum inherits the spectral properties of the driving fields.

For sake of comparison, the theoretical prediction of the FWM is provided in figure 2(c). The calculations have been performed by exploiting the *split step Fourier* method [38] for numerically solving the nonlinear propagation equation of the electric field $\mathbf{E}(\mathbf{r}, t) = \mathbf{A}_1(z, t)e^{i(k_1 z - \omega_1 t)} + \mathbf{A}_2(z, t)e^{i(k_2 z - \omega_2 t)} + \mathbf{A}_3(z, t)e^{i(k_3 z - \omega_3 t)}$, where the index $j = 1, 2, 3$ refers to the three pulses involved in the process (800 nm, near-IR and FWM pulses), $\mathbf{A}_j$ is the corresponding complex envelope, k_j is the component of the wavevector along the propagation direction z, and ω_j the central frequency of the pulses. The experiment has been modeled by using a set of three coupled equations, in the form of $\partial\mathbf{A}_j(z, t)/\partial z + \mathcal{D}\mathbf{A}_j(z, t) = -(\mu_0\omega_j^2/2ik_j)\mathbf{p}_j(z, t)$, where $\mathbf{p}_j$ is the nonlinear dipole moment density including the main third-order contributions affecting the experiment, i.e. SPM, XPM and FWM; $\mathcal{D}$ is the dispersion operator in the time domain. The simulated FWM spectra show a reasonable agreement with the measured ones both in terms of delay-dependence and spectral intensity. The calculated FWM pulse energy assesses on tens-of-μJ-level that matches with the experimental results. In particular, an output energy of 11 μJ (conversion efficiency from the 800 nm pump to the FWM of $\approx$5%) was measured compared to a predicted value of 20 μJ.

FWM generation can be optimized by changing the gas type and pressure [23, 39]. In this work, we used the same experimental configuration for investigating molecular gases, including N_2 and CO_2. The main results achieved in CO_2-filled HCF under the same conditions as in Kr are shown in figure 3. Figure 3(a) reports the evolution of the 800 nm spectrum and of the newly generated FWM spectrum as a function of the delay between the two input fields. The 800 nm components is affected by a remarkable modulation at negative delays. This long-lasting modulation is due to additional effects that occur when molecular gases are excited by intense ultrashort pulses, namely the activation of roto-vibrational dynamics that are associated to a transient birefringence of the molecules according to the polarization axis of the driving field [40, 41]. In this case, a comparison between the measured and the computed FWM spectra is

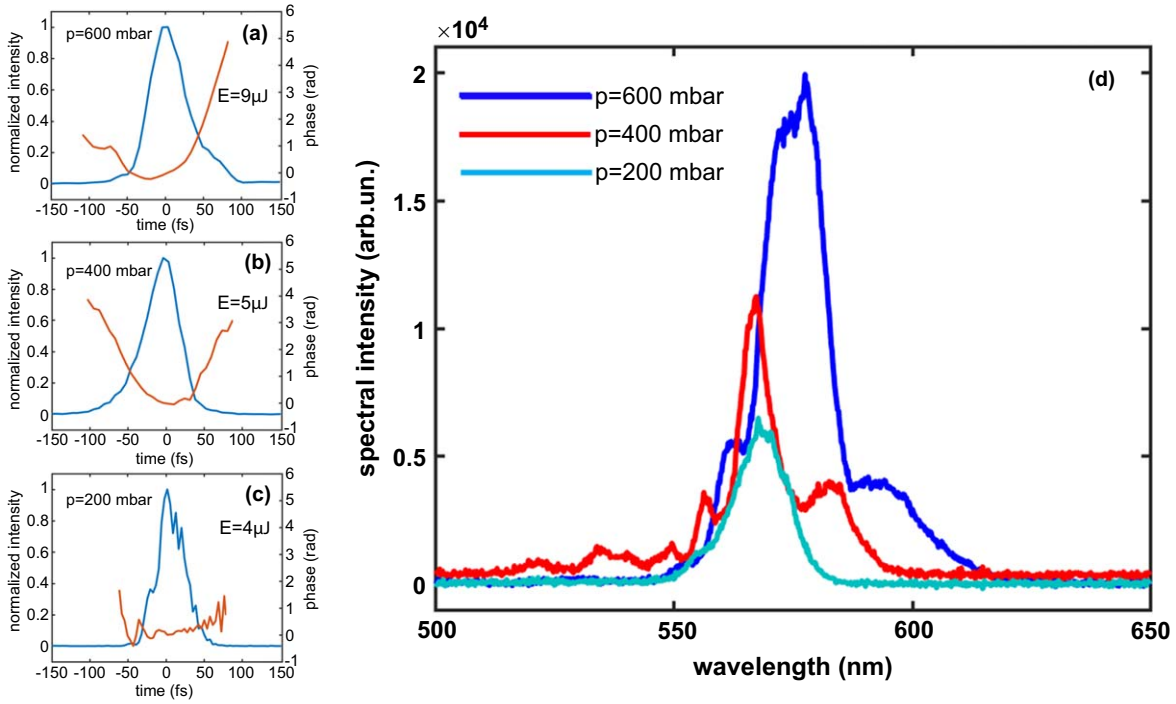

Figure 4. FWM pulse temporal characterization at (a) $p = 600$ mbar, (b) $p = 400$ mbar and (c) $p = 200$ mbar. The pulse energy corresponding to each pressure value is also reported. (d) Pressure dependence of the FWM spectra.

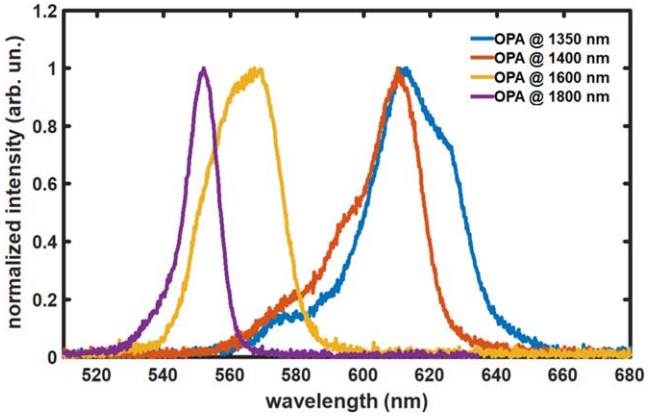

Figure 5. FWM spectral tunability as a function of the OPA pulse central wavelength.

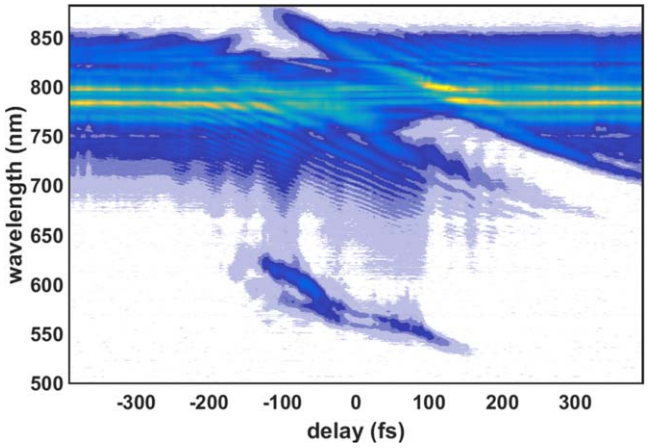

Figure 6. FWM generation in Kr by using a chirped 800 nm pulse.

provided in figures 3(b) and (c). With respect to Kr, an efficient generation of nonlinear components centered at 580nm was observed in CO_2. Compared to the the Kr case, the difference in the spectral position of the FWM contribution must be attributed to the strong perturbation of the driving pulse spectra due to the above mentioned roto-vibrational dynamics.

A temporal characterization of the FWM signal was performed by means of the FROG technique. A 50 μm BBO crystal is used for generating the second-harmonics (SH) of two delayed replica of the FWM pulse. A collection of SH spectra were acquired as a function of the delay between the replica and subsequently used for retrieving the temporal profile of the FWM pulse. As reported in figure 3(d), a 45 fs pulse envelope was obtained. The phase of the reconstructed pulse shows a quadratic dependence that can be potentially compensated by means of chirped mirrors, thus reducing the pulse duration to 30 fs. The simulated FWM spectra shown in figure 3(c) exhibit a larger bandwidth which can support even shorter durations, down to 17 fs. The mismatch between the experimental and the numerical results can be attributed to the delay-dependence of the wave mismatch vector and of the molecular hyperpolarizability produced by the roto-vibrational dynamics experienced by CO_2 molecules under the effects of intense ultrashort pulses [42, 43], which was not taken into account in our simulations and that can play a role in shaping the FWM spectrum.

In CO_2, we obtained the same FWM energy as in Kr. Since both the conversion efficiency and the spectral distribution exhibited a significant dependence on the amount of gas contained inside the fiber, the output energy and the pulse duration were measured for different gas pressures. The

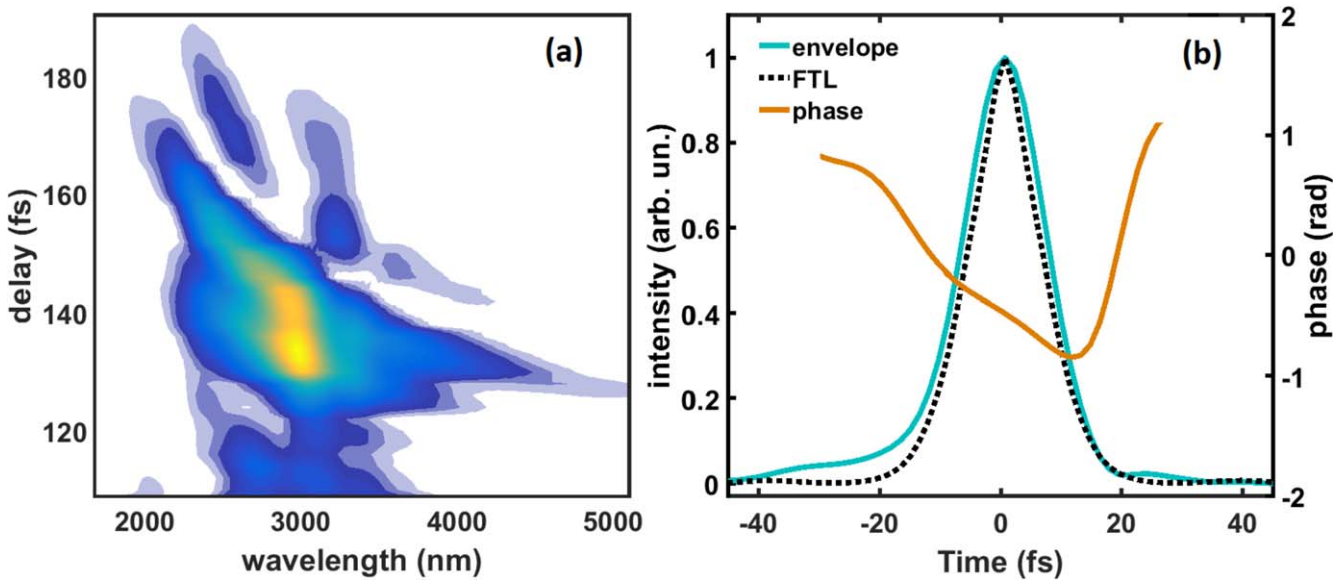

Figure 7. Numerical investigation on FWM generation in the mid-IR. (a) A broadband spectrum of mid-IR components centered around 3.1 μm is predicted. (b) The simulations predict mid-IR pulses with a FWHM of 15 fs, corresponding to sub-two optical cycles.

results obtained by changing the pressure at a fixed delay are provided in figure 4. It is possible to observe that as the pressure decreases from 600 to 200 mbar both the intensity and the bandwidth of the FWM signal decrease. At higher pressures, SPM and roto-vibrational-induced phase-modulation are stronger. These processes produce a significant spectral broadening of the interacting pulses making more components available for the frequency mixing process. On the other hand, these phenomena introduce a nonlinear perturbation of the phase that is responsible for a temporal dispersion of the interacting fields. As a consequence, the resulting duration of the FWM pulses decreases from 70 fs down to 39 fs by reducing the pressure from 600 to 200 mbar. In this framework, the performances of HCF-based FWM would possibly benefit from the phase-shaping of the input pulses, allowing for a pre-compensation of phase-distortion effects during the interaction in the HCF.

In our configuration, an additional factors limiting the conversion efficiency is represented by the mismatch between the driving pulses durations. According to calculations, a significant enhancement in the conversion efficiency is expected by using shorter 800 nm pulses. In particular, by reducing the pulse duration to the same scale of the OPA pulses, energy of $\approx$40 μJ can be attained. Moreover, by scaling the energy of the driving sources towards the mJ level, higher FWM energies can be potentially achieved. In this case, HCF with a larger inner diameter must be used, in order to reduce the gas ionization. A more sophisticated analytical model is also required to account for the effects of ionization [39].

By operating the OPA at different wavelengths, the FWM signal can be tuned, as shown in figure 5. Here, several FWM spectra are reported, each of which was acquired at a different OPA central wavelength. By changing the OPA wavelength from 1.35 to 1.8 μm the FWM spectrum undergoes a shift from 530 to 650 nm. The bandwidth of the FWM spectrum reduces at 1.8 μm. This can be attributed to a decrease of the OPA spectral bandwidth while approaching the longer wavelengths.

An alternative way for a spectral tuning of the FWM is based on the introduction of a temporal dispersion into one of the two driving pulses. In this case, only those spectral components of the chirped pulse that are temporally overlapped with the second pulse contribute to the process. By changing the delay between the two pulses, different components can be selected, thus leading to the possibility of finely tuning the FWM frequency. The measurement shown in figure 6 was performed under the same experimental conditions as in figure 2 by adding a phase distortion to the 800 nm pulses. Filamentation in an Ar-filled gas cell was used for phase shaping [44, 45]. Uncompressed positively-chirped 120 fs pulses at 800 nm were thus obtained. The advantage of exploiting filamentation relies in the possibility it offers of achieving both phase dispersion and spectral broadening. As a consequence, more components are available during the FWM process and a larger tunability range can be achieved. As expected, the FWM spectrum experiences a drift as a function of the delay. At each delay, the bandwidth of the FWM signal is narrower than that obtained in the transform-limited pulse configuration since only a selection of 800 nm pulse spectrum is taking part into the mixing process due to the temporal spreading of its components. In this scheme, the FWM pulses energy decreases to below 1 μJ.

A future application of our HCF-based FWM scheme will be the generation of ultrashort pulses in the mid-IR. According to a numerical investigation, phase-matching for the frequency conversion process $\omega_3 = 2\omega_2 - \omega_1$ is enabled under a high gas pressure regime ($>$ 4.5 bar). By setting the OPA operational wavelength at 1.3 μm FWM generation of a seed radiation at around 3.1 μm can be achieved (see figure 7). The conversion efficiency is expected to be one order of magnitude lower than that obtained for FWM in the

Table 1. State of the art in high-energy linear source of ultrashort pulses based on the OPA/OPCPA and FWM schemes.

Process (NL media)[a]	Pump sources	Output pulses			Conversion efficiency[e]	Main references
		$\lambda(\mu m)$[b]	τ(fs)[c]	E(μJ)[d]		
FWM in the UV						
gas (gas-filled HCF and filaments)	few-mJ tens-fs Ti:Sa+SH/TH[f] SH+OPA in the IR	0.16–0.3	<10–30	1–10	0.1%–30%	[22–25]
FWM in the visible						
bulk (fused silica, sapphire)	few-mJ tens-fs Ti:Sa	400–700	30–50	1–3	<10%	[46, 47]
gas(air-, Ar- filament)	few-mJ tens-fs Ti:Sa+OPA in the IR	400–700	10–30	1–10	1%–20%	[26]
FWM in the mid-IR						
bulk(CaF_2, BaF_2)	few-mJ hundreds-fs Ti:Sa+near-IR OPA	2.4–7.7	200–300	0.1–0.2	<1%	[12]
gas(air-, N_2-, Ar- filament)	few-mJ hundreds-fs Ti:Sa+SH	2–6	<10–20	0.5–2	<1%	[27–29]
OPA in the vis						
(BBO)	few-mJ tens-fs SH of Ti:Sa	0.5–0.7	<10–25	10–500	20%–30%	[48, 49]
OPA in the near-IR						
(BBO)	few-mJ tens-fs Ti:Sa	1.3–2.2	15–200	500–1500	20%–30%	[4–6]
OPCPA in the near-IR						
(BBO, KTP, BiB_3O_6, PPMgLN, $LiNbO_3$)	mJ ps and fs solid-state (Nd:YAG, Nd:YLF, Yb-doped LPF, Ti:Sa)	1.5–2.1	10–50	60–3000	18%–25%	[9, 50–52]
OPCPA in the mid-IR						
(ZGP, PPLN, KTA $KNbO_3$, MgO:$LiNbO_3$)	multi-mJ ps fiber-doped (Ho:YLF) or solid-state (Nd:YVO_4, Nd:YAG)	2–7	10–200	12–10000	10%–24%	[7, 8, 10, 11]

[a] Nonlinear (NL) media.
[b] Spectral range containing the central wavelengths of the referenced sources.
[c] Range of the pulse durations of the referenced sources.
[d] Range of the pulse energy of the referenced sources.
[e] For FWM process, the efficiency is estimated as the ratio between the FWM pulse (ω_3) energy and the pump pulse (ω_1) energy; in the case of OPA and OPCPA, it is estimated as the ratio between the signal pulse energy and the pump pulse energy (the idler is neglected).
[f] (SH) second harmonic and (TH) third harmonic of the output pulses of a Ti:Sa system.

visible. This is due both to enhanced fiber losses at longer wavelengths and to a detrimental velocity mismatch among the propagating pulses. A broadband spectrum is however predicted, potentially supporting 15 fs pulse duration, on the single-optical-cycle time scale.

It is worth to briefly comment on the results here reported in comparison with the state of the art in the field of high-energy (from the 1 μJ level upward) ultrashort (few-tens of fs) pulse generation by frequency conversion. To this purpose, a summary of the most remarkable results available in the literature is provided in table 1.

By inspection, it is possible to notice that both FWM-based sources and parametric amplifier cover a wide range of spectral regions, going from the UV to the mid-IR. Throughout the spectral range, OPAs and OPCPAs allows for unsurpassed performances, in terms of conversion efficiency and output pulse energy. This is mainly due to the availability of crystals with structured optical properties and highly nonlinear coefficients. Moreover, geometrical degrees of freedom are also available in OPAs and OPCPAs, making the non-collinear configuration the most widely used for achieving ultrabroadband phase-matching.

FWM provides an alternative way for achieving ultra-broadband μJ-level pulses by using more compact setups. In particular, FWM in gas media (gas-filled HCF and plasma filaments) enables good conversion efficiencies and allows to access pulse durations on the few-cycle scale, without any additional compression process as SPM. Our experiment aims at combining the advantages provided by gas-based FWM

with the long interaction distances supported by HCF. The output pulse energy and duration are on the level of the most intense ultrafast sources of visible light based on FWM.

3. Conclusions

The scheme we presented here provides the possibility to generate ultrashort pulses by frequency conversion of an intense two-color input field inside a gas-filled HCF. In particular, we reported on the observation of ≈10 μJ visible ultrashort pulses through FWM driven by two intense ultrashort IR pulses. The conversion efficiency we measured is quite low (FWM pulse energy over the pump 800 nm pulse energy, ≈5%) but an improvement can potentially be achieved by properly shaping the driving pulses duration and phases. By using the same scheme, frequency conversion in different portions of the spectrum can be achieved. Particularly attractive is the perspective to apply this approach to FWM generation in the mid-IR spectral domain. In this sense, calculations suggested a broadband frequency conversion resulting in sub-two-optical cycle pulses at 3.1 μm.

Acknowledgments

The research leading to these results has received funding from the European Research Council under the European Union's Seventh Framework Programme (FP7/2007-2013)/ERC Grant Agreement No. 307964 (UDYNI), from Laserlab-Europe (EU-H2020 654148), from the Italian Ministry of Research and Education (ELI project—ESFRI Roadmap), from Regione Lombardia through the project FEMTOTERA (ID: CONCERT2014-008) and from Fondazione Cariplo through the project GREENS (No. 2013-0656). This project has received funding from the European Union's Horizon 2020 research and innovation programme under the Marie Skodowska-Curie Grant Agreement Nos. 674960 (ASPIRE) and 641789 (MEDEA).

ORCID iDs

Anna G Ciriolo https://orcid.org/0000-0003-1189-329X
Michele Devetta https://orcid.org/0000-0002-3806-3475
Davide Faccialà https://orcid.org/0000-0002-5072-0394
Caterina Vozzi https://orcid.org/0000-0002-0212-0191
Salvatore Stagira https://orcid.org/0000-0002-8457-3185

References

[1] Pazourek R, Nagele S and Burgdörfer J 2015 Attosecond chronoscopy of photoemission *Rev. Mod. Phys.* **87** 765
[2] Brida D, Manzoni C, Cirmi G, Marangoni M, Bonora S, Villoresi P, De Silvestri S and Cerullo G 2009 Few-optical-cycle pulses tunable from the visible to the mid-infrared by optical parametric amplifiers *J. Opt.* **12** 013001
[3] Ciriolo A G, Negro M, Devetta M, Cinquanta E, Faccialà D, Pusala A, De Silvestri S, Stagira S and Vozzi C 2017 Optical parametric amplification techniques for the generation of high-energy few-optical-cycles IR pulses for strong field applications *Appl. Sci.* **7** 265
[4] Vozzi C, Calegari F, Benedetti E, Gasilov S, Sansone G, Cerullo G, Nisoli M, De Silvestri S and Stagira S 2007 Millijoule-level phase-stabilized few-optical-cycle infrared parametric source *Opt. Lett.* **32** 2957–9
[5] Hauri C P *et al* 2007 Intense self-compressed, self-phase-stabilized few-cycle pulses at 2 μm from an optical filament *Opt. Lett.* **32** 868–70
[6] Schmidt B E, Shiner A D, Lassonde P, Kieffer J-C, Corkum P B, Villeneuve D M and Légaré F 2011 CEP stable 1.6 cycle laser pulses at 1.8 μm *Opt. Express* **19** 6858–64
[7] Andriukaitis G, Balčiūnas T, Ališauskas S, Pugžlys A, Baltuška A, Popmintchev T, Chen M-C, Murnane M M and Kapteyn H C 2011 90 GW peak power few-cycle mid-infrared pulses from an optical parametric amplifier *Opt. Lett.* **36** 2755–7
[8] Mayer B W, Phillips C R, Gallmann L, Fejer M M and Keller U 2013 Sub-four-cycle laser pulses directly from a high-repetition-rate optical parametric chirped-pulse amplifier at 3.4 μm *Opt. Lett.* **38** 4265–8
[9] Shamir Y, Rothhardt J, Hädrich S, Demmler S, Tschernajew M, Limpert J and Tünnermann A 2015 High-average-power 2 μm few-cycle optical parametric chirped pulse amplifier at 100 khz repetition rate *Opt. Lett.* **40** 5546–9
[10] Sanchez D, Hemmer M, Baudisch M, Cousin S L, Zawilski K, Schunemann P, Chalus O, Simon-Boisson C and Biegert J 2016 7 μm, ultrafast, sub-millijoule-level mid-infrared optical parametric chirped pulse amplifier pumped at 2 μm *Optica* **3** 147–50
[11] Elu U, Baudisch M, Pires H, Tani F, Frosz M H, Köttig F, Ermolov A, Russell P S J and Biegert J 2017 High average power and single-cycle pulses from a mid-IR optical parametric chirped pulse amplifier *Optica* **4** 1024–9
[12] Nienhuys H-K, Planken P C M, van Santen R A and Bakker H J 2001 Generation of mid-infrared pulses by $\chi^{(3)}$ difference frequency generation in Ca_{F2} and Ba_{F2} *Opt. Lett.* **26** 1350–2
[13] Crespo H, Mendonça J T and Santos A D 2000 Cascaded highly nondegenerate four-wave-mixing phenomenon in transparent isotropic condensed media *Opt. Lett.* **25** 829–31
[14] Kobayashi T, Liu J and Kida Y 2012 Generation and optimization of femtosecond pulses by four-wave mixing process *IEEE J. Sel. Top. Quantum Electron.* **18** 54–65
[15] Weigand R and Crespo H M 2015 Fundamentals of highly non-degenerate cascaded four-wave mixing *Appl. Sci.* **5** 485–515
[16] Varillas R B, Candeo A, Viola D, Garavelli M, De Silvestri S, Cerullo G and Manzoni C 2014 Microjoule-level, tunable sub-10 fs UV pulses by broadband sum-frequency generation *Opt. Lett.* **39** 3849–52
[17] Hill K O, Johnson D C, Kawasaki B S and MacDonald R I 1978 CW three-wave mixing in single-mode optical fibers *J. Appl. Phys.* **49** 5098–106
[18] Inoue K and Toba H 1992 Wavelength conversion experiment using fiber four-wave mixing *IEEE Photonics Technol. Lett.* **4** 69–72
[19] Washio K, Inoue K and Kishida S 1980 Efficient large-frequency-shifted three-wave mixing in low dispersion wavelength region in single-mode optical fibre *Electron. Lett.* **16** 658–60
[20] Sharping J E, Fiorentino M, Coker A, Kumar P and Windeler R S 2001 Four-wave mixing in microstructure fiber *Opt. Lett.* **26** 1048–50

[21] Li Y H, Zhao Y Y and Wang L J 2012 Demonstration of almost octave-spanning cascaded four-wave mixing in optical microfibers *Opt. Lett.* **37** 3441–3
[22] Durfee C G, Backus S, Kapteyn H C and Murnane M M 1999 Intense 8-fs pulse generation in the deep ultraviolet *Opt. Lett.* **24** 697–9
[23] Misoguti L, Backus S, Durfee C G, Bartels R, Murnane M M and Kapteyn H C 2001 Generation of broadband VUV light using third-order cascaded processes *Phys. Rev. Lett.* **87** 013601
[24] Zuo P, Fuji T and Suzuki T 2010 Spectral phase transfer to ultrashort UV pulses through four-wave mixing *Opt. Express* **18** 16183–92
[25] Beutler M, Ghotbi M, Noack F and Hertel I V 2010 Generation of sub-50-fs vacuum ultraviolet pulses by four-wave mixing in argon *Opt. Lett.* **35** 1491–3
[26] Théberge F, Aközbek N, Liu W, Becker A and Chin S L 2006 Tunable ultrashort laser pulses generated through filamentation in gases *Phys. Rev. Lett.* **97** 023904
[27] Fuji T and Suzuki T 2007 Generation of sub-two-cycle mid-infrared pulses by four-wave mixing through filamentation in air *Opt. Lett.* **32** 3330–2
[28] Fuji T and Nomura Y 2013 Generation of phase-stable sub-cycle mid-infrared pulses from filamentation in nitrogen *Appl. Sci.* **3** 122–38
[29] Voronin A A, Nomura Y, Shirai H, Fuji T and Zheltikov A 2014 Half-cycle pulses in the mid-infrared from a two-color laser-induced filament *Appl. Phys.* B **117** 611–9
[30] Cook D J and Hochstrasser R M 2000 Intense terahertz pulses by four-wave rectification in air *Opt. Lett.* **25** 1210–2
[31] Bartel T, Gaal P, Reimann K, Woerner M and Elsaesser T 2005 Generation of single-cycle thz transients with high electric-field amplitudes *Opt. Lett.* **30** 2805–7
[32] Brée C, Demircan A and Steinmeyer G 2011 Saturation of the all-optical kerr effect *Phys. Rev. Lett.* **106** 183902
[33] Vozzi C, Manzoni C, Calegari F, Benedetti E, Sansone G, Cerullo G, Nisoli M, De Silvestri S and Stagira S 2008 Characterization of a high-energy self-phase-stabilized near-infrared parametric source *J. Opt. Soc. Am.* B **25** B112–7
[34] Augst S, Meyerhofer D D, Strickland D and Chin S-L 1991 Laser ionization of noble gases by coulomb-barrier suppression *J. Opt. Soc. Am.* B **8** 858–67
[35] Shelton D P and Rice J E 1994 Measurements and calculations of the hyperpolarizabilities of atoms and small molecules in the gas phase *Chem. Rev.* **94** 3–29
[36] Islam M N, Simpson J R, Shang H T, Mollenauer L F and Stolen R H 1987 Cross-phase modulation in optical fibers *Opt. Lett.* **12** 625–7
[37] Agrawal G P, Baldeck P L and Alfano R R 1989 Temporal and spectral effects of cross-phase modulation on copropagating ultrashort pulses in optical fibers *Phys. Rev.* A **40** 5063
[38] Agrawal G P 2007 *Nonlinear Fiber Optics* (New York: Academic)
[39] Durfee C G, Misoguti L, Backus S, Kapteyn H C and Murnane M M 2002 Phase matching in cascaded third-order processes *J. Opt. Soc. Am.* B **19** 822–31
[40] Bartels R A, Weinacht T C, Wagner N, Baertschy M, Greene C H, Murnane M M and Kapteyn H C 2001 Phase modulation of ultrashort light pulses using molecular rotational wave packets *Phys. Rev. Lett.* **88** 013903
[41] Calegari F, Vozzi C and Stagira S 2009 Optical propagation in molecular gases undergoing filamentation-assisted field-free alignment *Phys. Rev.* A **79** 023827
[42] Bartels R A, Wagner N L, Baertschy M D, Wyss J, Murnane M M and Kapteyn H C 2003 Phase-matching conditions for nonlinear frequency conversion by use of aligned molecular gases *Opt. Lett.* **28** 346–8
[43] Hartinger K, Nirmalgandhi S, Wilson J and Bartels R A 2005 Efficient nonlinear frequency conversion with a dynamically structured nonlinearity *Opt. Express* **13** 6919–30
[44] Hauri C P, Kornelis W, Helbing F W, Heinrich A, Couairon A, Mysyrowicz A, Biegert J and Keller U 2004 Generation of intense, carrier-envelope phase-locked few-cycle laser pulses through filamentation *Appl. Phys.* B **79** 673–7
[45] Odhner J and Levis R J 2012 Direct phase and amplitude characterization of femtosecond laser pulses undergoing filamentation in air *Opt. Lett.* **37** 1775–7
[46] Liu J and Kobayashi T 2009 Generation of μj multicolor femtosecond laser pulses using cascaded four-wave mixing *Opt. Express* **17** 4984–90
[47] Liu J and Kobayashi T 2009 Wavelength-tunable, multicolored femtosecond-laser pulse generation in fused-silica glass *Opt. Lett.* **34** 1066–8
[48] Tzankov P, Zheng J, Mero M, Polli D, Manzoni C and Cerullo G 2006 300 μj noncollinear optical parametric amplifier in the visible at 1 khz repetition rate *Opt. Lett.* **31** 3629–31
[49] Odhner J H and Levis R J 2015 High-energy noncollinear optical parametric amplifier producing 4 fs pulses in the visible seeded by a gas-phase filament *Opt. Lett.* **40** 3814–7
[50] Mücke O D, Ališauskas S, Verhoef A J, Pugžlys A, Baltuška A, Smilgevičius V, Pocius J, Giniūnas L, Danielius R and Forget N 2009 Self-compression of millijoule 1.5 μm pulses *Opt. Lett.* **34** 2498–500
[51] Gu X *et al* 2009 Generation of carrier-envelope-phase-stable 2-cycle 740-μj pulses at 2.1- μm carrier wavelength *Opt. Express* **17** 62–9
[52] Yin Y, Li J, Ren X, Zhao K, Wu Y, Cunningham E and Chang Z 2016 High-efficiency optical parametric chirped-pulse amplifier in $BiB3O_6$ for generation of 3 mJ, two-cycle, carrier-envelope-phase-stable pulses at 1.7 μm *Opt. Lett.* **41** 1142–5